anatomia

MDPI

Article

Macroscopic Anatomy of the Stifle Joint in the Pampa's Deer (*Ozotoceros bezoarticus*-Linnaeus, 1758)

Horst Erich König [1], Sokol Duro [2,*] and William Pérez [3]

[1] Institut für Morphologie der Veterinärmedizinischen Universität Wien, A-1210 Wien, Austria; horst.koenig@vetmeduni.ac.at
[2] Faculty of Veterinary Medicine, Agricultural University of Tirana, 1000 Tirana, Albania
[3] Unidad de Anatomía, Facultad de Veterinaria, Universidad de la República, Ruta 8, Km 18, Montevideo 13000, Uruguay; vetanat@gmail.com
* Correspondence: durosokol@ubt.edu.al

Abstract: The objective of this paper was to describe the anatomy of the stifle joint (*Articulatio genus*) of the pampas deer (*Ozotoceros bezoarticus*, Linnaeus, 1758) by dissection and imaging studies. Twenty-six pelvic limbs were used for gross dissection, and four stifle regions from two animals were used for radiography and magnetic resonance imaging (MRI). The stifle joint of the pampas deer comprised the femoropatellar joint (joint between the distal part of the femur and the patella), and the femorotibial joint joined the femoral condyles to the proximal extremity of the tibia. The general anatomy of the stifle joint, including the overall morphology of the joint with its bones, complementary parts, means of attachment, and anatomical relationships, was like that of other ruminant species of similar size. Imaging techniques such as MRI allow adequate visualization of most components of the stifle joint.

Keywords: anatomy; arthrology; Cervidae; deer; ruminants; stifle joint

Citation: König, H.E.; Duro, S.; Pérez, W. Macroscopic Anatomy of the Stifle Joint in the Pampa's Deer (*Ozotoceros bezoarticus*-Linnaeus, 1758). *Anatomia* **2023**, 2, 124–137. https://doi.org/10.3390/anatomia2020012

Academic Editor: Francesco Fornai

Received: 10 March 2023
Revised: 31 March 2023
Accepted: 19 April 2023
Published: 23 April 2023

1. Introduction

Natively living ruminants have been found on all continents except Antarctica and Oceania; currently, most species are found in Africa and Eurasia [1]. Most ruminants are Bovids and Cervids, with the majority being Cervids [2,3]. Cervids are found in South America and Bovids are found in the wild.

Cervidae is a family of the Order Artiodactyla, included in the Infraorder Pecora of the Suborder Ruminantia. The pampas deer (*Ozotoceros bezoarticus*, Linnaeus, 1758) is the only species of the genus Ozotoceros with two subspecies found in Uruguay, *Ozotoceros bezoarticus arerunguaensis* and *Ozotoceros bezoarticus uruguayensis*, represented respectively by the populations of El Tapado and Sierra de Los Ajos in Uruguay [4]. The pampas deer is considered by the IUCN (International Union for Conservation of Nature and Natural Resources) as a near-threatened species [5], with the possibility of entering the vulnerable category soon. Scientific knowledge of endangered ruminants is fundamental, especially for the management of species in captivity. Despite this, basic information is often lacking for many species.

Ozotoceros bezoarticus deer are medium-sized animals, with males being slightly larger than females [6]. In wild populations, males reach a length of 130 cm (from the apex of the nose to the root of the tail), a height of 75cm at the withers, a tail length of 15 cm, and a weight approximately 35 kg [6]. However, data obtained from animals raised in semi-captivity indicate a somewhat smaller size [7].

The pampas deer is a relatively lightweight animal and a fast runner, averaging 20 to 30 miles per hour (on rare occasions, the top speed may reach 35 or 40 miles per hour), although it can only run for short periods of time before becoming fatigued. The life of the pampas deer in wetlands and flooded lands has developed their ability to run with

high jumps but also to swim, using mainly their hind legs for powerful propulsion when running or jumping [8].

Most anatomical studies related to pampas deer have focused on their reproductive organs [9–12], digestive system [13–15], and cardiovascular system [16–20]. There are still many organs to be investigated, especially in the locomotor apparatus, where there is an absence of descriptions.

Studies concerning joints are very scarce. Allen et al. [21] reviewed the macroscopic anatomy of the sheep stifle joint, and there are detailed descriptions in classical textbooks [22–24]. Magnetic resonance imaging (MRI) would provide additional information on bone and soft tissue injuries when compared to current imaging techniques such as radiography and ultrasonography, which provide limited information [25,26]. In addition, tendons and ligaments are more distinguishable by MRI than by computed tomography (CT) or ultrasonography [27,28]. An MRI for the study of this joint in sheep was published by Vandeweerd et al. [29]. Regarding arthrology, very little information has been published on deer species. Shigue et al. [30] studied the stifle joint in marsh deer by dissection, radiography, CT, and MRI.

Based on the literature so far, the latter investigations provide the only information on the macroscopic anatomy of the stifle joint in cervids. Therefore, the objective of this study was to describe the anatomical features of this joint in animals of the genus *Ozotoceros*, by macroscopic dissection, radiography, and MRI.

2. Materials and Methods

The study was carried out with 15 pampas deer species (*Ozotoceros bezoarticus* spp.) dead from natural causes and free from obvious pathologies of the locomotor system from the Estación de Cría de Fauna Autóctona de Pan de Azúcar (ECFA, Maldonado, Uruguay). Of these animals, 10 were adult females over two years old, and five were juveniles younger than one year (three males and two females). The mean body mass of the adult females (n = 10) was 14.5 $\pm$ 2.4 kg, and that of the young animals (n = 5) was 4.2 $\pm$ 1.3 kg. The dead animals at the ECFA were collected by local personnel and frozen at -20 °C, then transferred and dissected at the anatomy laboratory of the Veterinary College.

The animals were weighed and measured and then 13 animals (26 pelvic limbs) were dissected. The animals were studied by simple dissection or with the use of a binocular loupe. First, the pelvic limb was removed by incising the coxofemoral joint (*Articulatio coxae*), and both the femur and the tibia were sectioned by half of their length to proceed with the isolation of the stifle region and adjacent parts. By means of dissection, the structures that acted as means of union (tendons, joint capsule, ligaments), menisci, and in the last stage, the bony parts participating in the joint, were dissected and cleaned. During and after each stifle dissection, a detailed description of the structures, such as the articular surfaces of the participating bones, the complementary formations, and the means of the union of these joints, was also carried out.

Four stifle regions from two adult animals were used for the imaging studies: two for radiography and two others for MRI. The radiographs were taken at the Veterinary School using a Vetter-Rems fixed radiology device with a Carestream digitizer, and the MRIs were taken at the Hospital de Clínicas of the Universidad de la República, with a Siemens 1.5 tesla resonator. The stifles of these two animals were subsequently dissected and sectioned longitudinally (sagittally) to compare with the radiological and MRI images obtained.

All data pertaining to each animal and observations made during dissection were recorded in individual spreadsheets for each specimen. As the dissections progressed, photographs were taken with a Nikon D7100 digital camera. Each photograph was accompanied by an outline indicating the exact structures photographed. After downloading the photographs to the computer, they were filed in exclusive folders for each animal.

The nomenclature of the online version of the Nomina Anatomica Veterinaria [31] and their illustrated version [32] were used for the description.

3. Results

The stifle joint of the pampas deer is a composite, incongruent hinge joint as in other ruminants, comprised of the femoropatellar joint (*Articulatio femoropatellaris*) (joint between the distal part of the femur and the patella) and the femorotibial joint (*Articulatio femorotibialis*) that joined the femoral condyles to the proximal extremity of the tibia.

3.1. Articular Surfaces

From the two condyles of the distal part of the femur, the lateral one (*Condylus lateralis*) was larger than the medial (*Condylus medialis*).

The femoral trochlea (*Trochlea ossis femoris*) (Figure 1) responded to the patella by having a deep articular surface located between two prominent reliefs or lips that were almost equal. The medial and lateral condyles were located caudally on the distal end of the femur, and the lateral one was more developed. The two condyles (Figure 2) were separated by the intercondylar fossa (*Fossa intercondylaris*), which was very large and deep and terminated caudoproximally at the intercondylar line. The abaxial side of each condyle had a respective relief called the epicondyle.

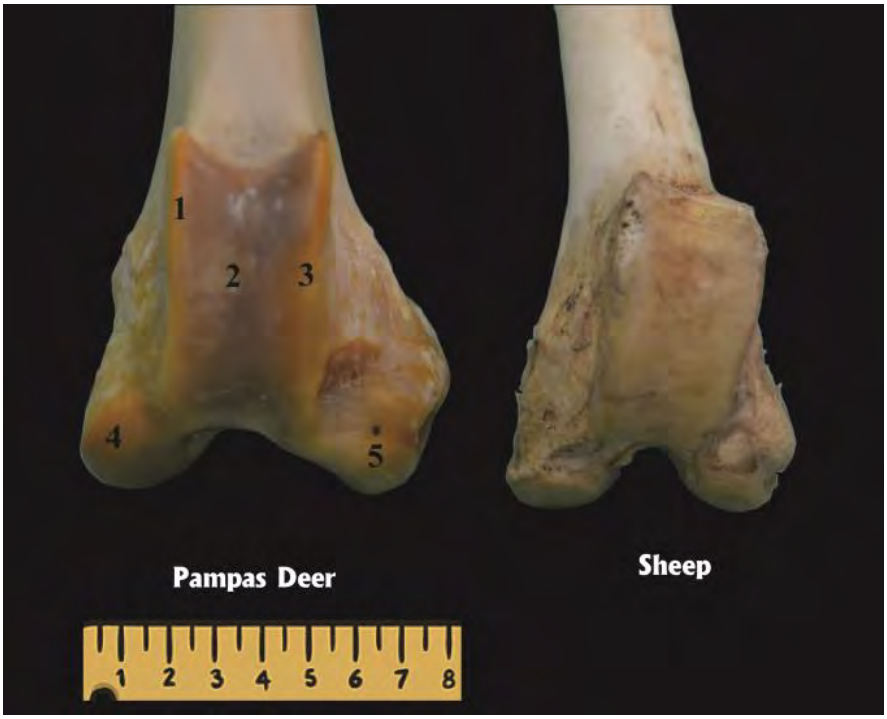

Figure 1. Distal extremity of the left femur of the pampas deer and sheep, cranial view. (**1**): Medial lip of femoral trochlea; (**2**): femoral trochlea, central depression; (**3**): lateral lip of femoral trochlea; (**4**): medial condyle; (**5**): lateral condyle.

The patella is opposed to the femoral trochlea and has an articular surface composed of two undulated parts, lateral and medial, separated by a little marked intermediate relief. The medial surface was wider than the lateral surface (Figure 3).

The tibia had the two tibial condyles (medial and lateral) proximally. Both were weakly concave from one side to the other and somewhat convex from cranial to caudal. The medial condyle was broader, and both were elevated against the intercondylar eminence. Both condyles were separated by the cranial, central (dividing the intercondylar area), and caudal intercondylar areas. (Figure 4)

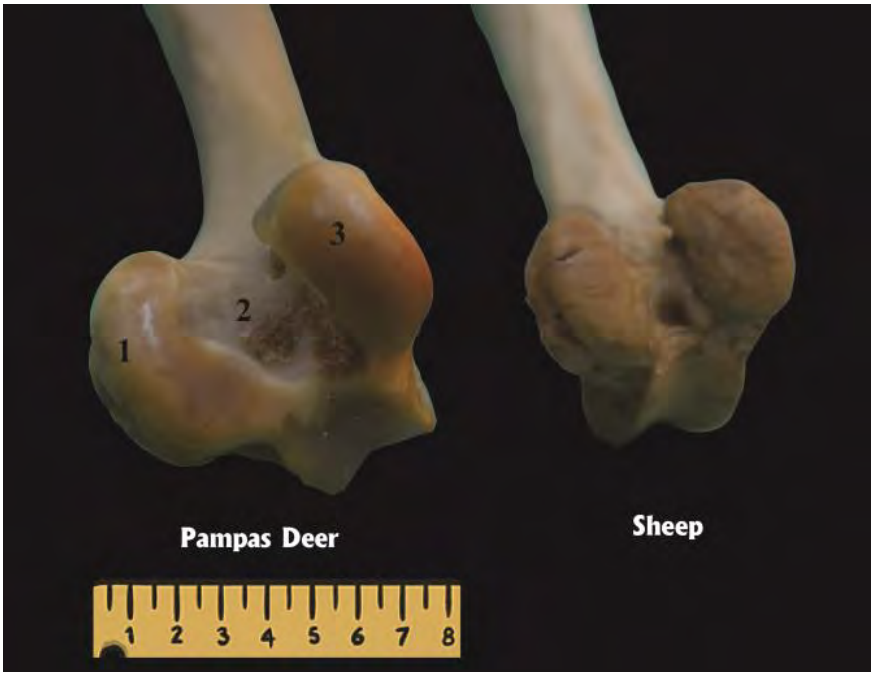

Figure 2. Distal extremity of the left femur of pampas deer and sheep, caudal view. (**1**): Lateral condyle; (**2**): intercondylar fossa; (**3**): medial condyle.

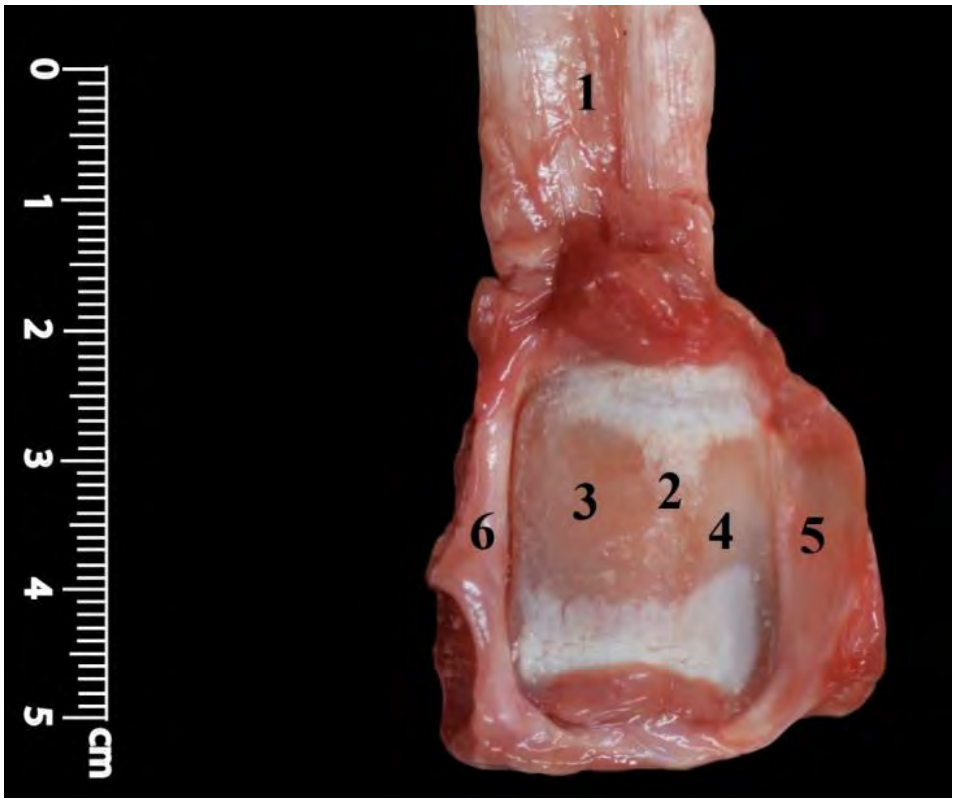

Figure 3. Caudal view of the articular surface of the left patella of the pampas deer. (**1**): Patellar ligament; (**2**): medial relief; (**3**): medial articular surface; (**4**): lateral articular surface; (**5**): lateral parapatellar fibrocartilage; (**6**): medial parapatellar fibrocartilage.

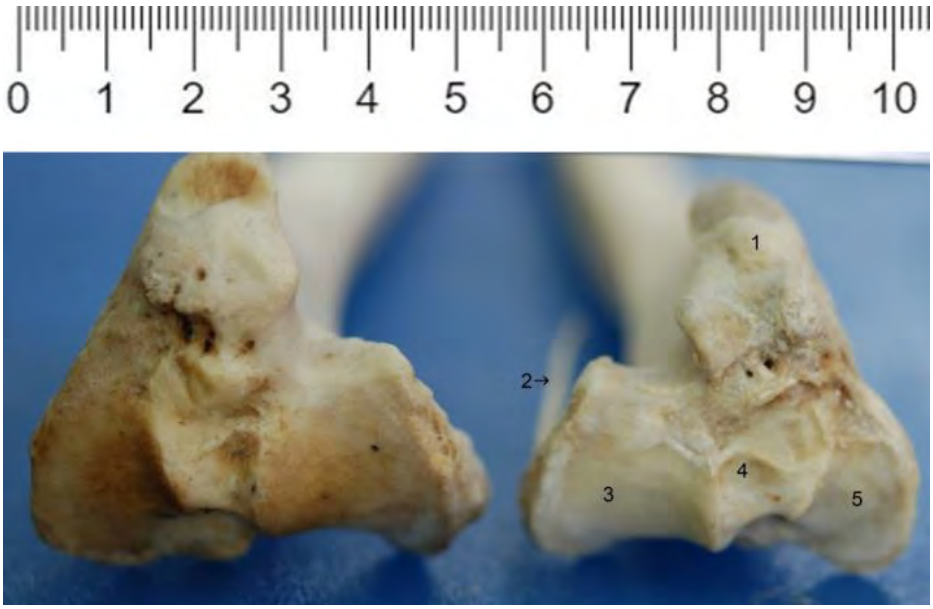

Figure 4. Proximal extremity of the tibia of the pampas deer, dorsal view. (**1**): Tibia tuberosity; (**2**): fibula; (**3**): lateral condyle; (**4**): central intercondylar fossa; (**5**): medial condyle.

In the radiograph shown, the bones involved in the joint are clearly visible (Figure 5).

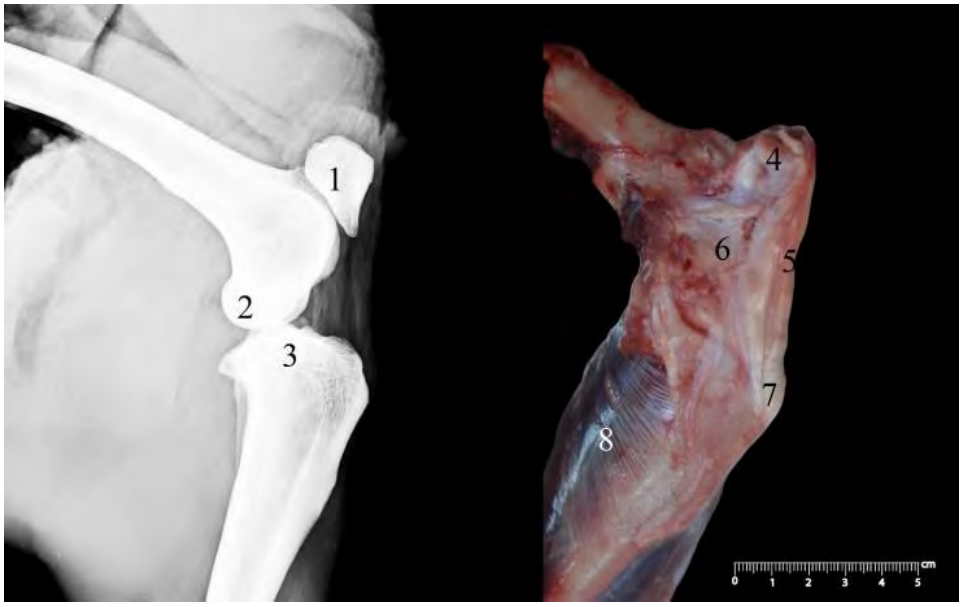

Figure 5. Left panel: plain radiograph of the left pelvic limb to show the bones involved in the stifle joint of the pampas deer. (**1**): Patella; (**2**): femoral condyle; (**3**); proximal extremity of tibia. **Right** panel: left pelvic limb, lateral view. (**4**): Patella; (**5**): patellar ligament; (**6**): articular capsule; (**7**): tibial tuberosity; (**8**): popliteus muscle.

3.2. Complementary Parts

The complementary parts include the two menisci interposed between the femoral and tibial condyles and the patellar fibrocartilaginous apparatus.

The lateral and medial menisci (*Meniscus medialis* and *Meniscus lateralis*) were fibrocartilaginous structures in a somehow semilunar shape (Figures 6 and 7). The medial was slightly narrower and less thickened than the lateral. Each meniscus had a convex lateral border, a concave and sharp medial border, a flat distal side, a concave proximal side, and

two extremities. Both menisci exposed the intercondylar eminence that was placed in the intercondylar fossa of the femur. The medial meniscus is inserted at its cranial pole into the cranial intercondylar area, cranial to the insertion of the opposite one, and at its caudal pole into the caudal intercondylar area. The lateral meniscus was inserted cranially closer to the intercondylar eminence. The cranial and caudal extremities of both menisci have no contact with each other, and the transverse ligament of the knee is not present.

Figure 6. Proximal view of the proximal extremity of the right tibia and its menisci in the pampas deer. (**1**): Extensor sulcus; (**2**): cranial part of the medial meniscus; (**3**): central part of the medial meniscus; (**4**): caudal insertion of the medial meniscus; (**5**): cranial cruciate ligament; (**6**): cranial insertion of the lateral meniscus; (**7**): central part of the lateral meniscus.

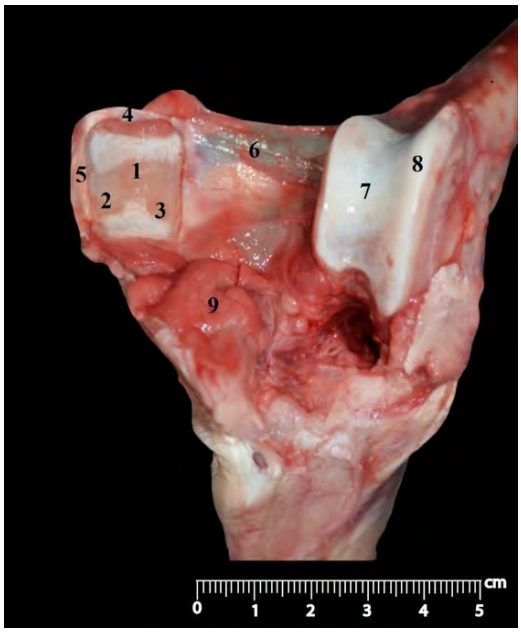

Figure 7. Cranial view after wide opening of the left stifle joint of the pampas deer. (**1**): Intermediate relief of the patellar articular surface; (**2**): lateral articular surface of the patella; (**3**): medial articular surface; (**4**): patellar insertion of the patellar ligament; (**5**): lateral parapatellar fibrocartilage; (**6**): synovial stratum of the patellofemoral joint capsule; (**7**): femoral trochlea; 8: lateral lip of the femoral trochlea; (**9**): infrapatellar adipose body.

The caudal horn of the lateral meniscus was thickened and divided into two parts, one going to the popliteal incisure of the tibia and the other constituting the meniscofemoral ligament (*Ligamentum meniscofemorale*) (Figure 8), which was inserted into the medio-caudal part of the intercondylar fossa, constituting a means of indirect femorotibial attachment. The lateral border of the lateral meniscus was crossed obliquely by the tendon of the popliteus muscle, which was in turn covered by the lateral collateral ligament (Figures 9 and 10).

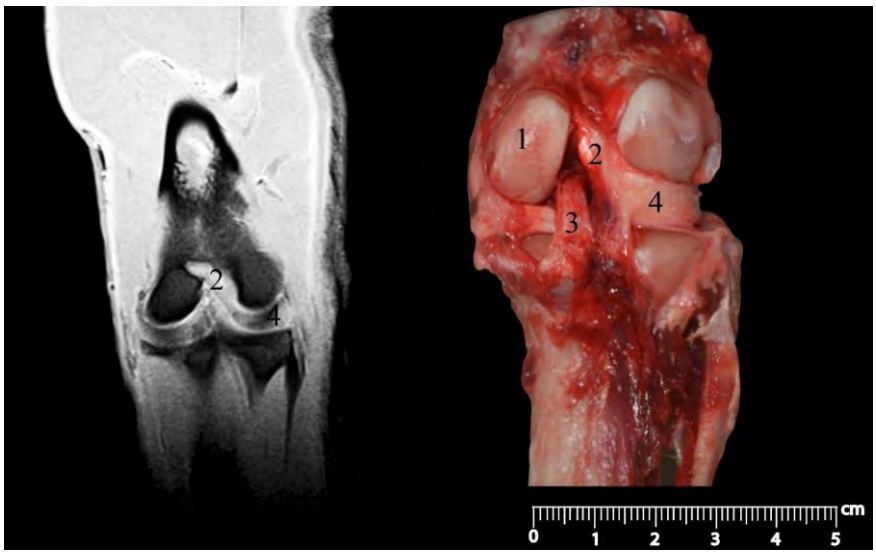

Figure 8. Left panel: MRI of the right stifle joint of the pampas deer, caudal view. (**2**): Meniscofemoral ligament; (**4**): lateral meniscus. **Right** panel: caudal view of the right stifle of the pampas deer after removal of the gastrocnemius muscles. (**1**): Medial condyle; (**2**): meniscofemoral ligament; (**3**): caudal cruciate ligament; (**4**): lateral meniscus.

Figure 9. Lateral view of the right thigh and leg of the pampas deer after removal of fasciae and gastrocnemius muscles. (**1**): Lateral collateral ligament; (**2**): tendon of the popliteus muscle; (**3**): tendon of the extensor digitorum longus.

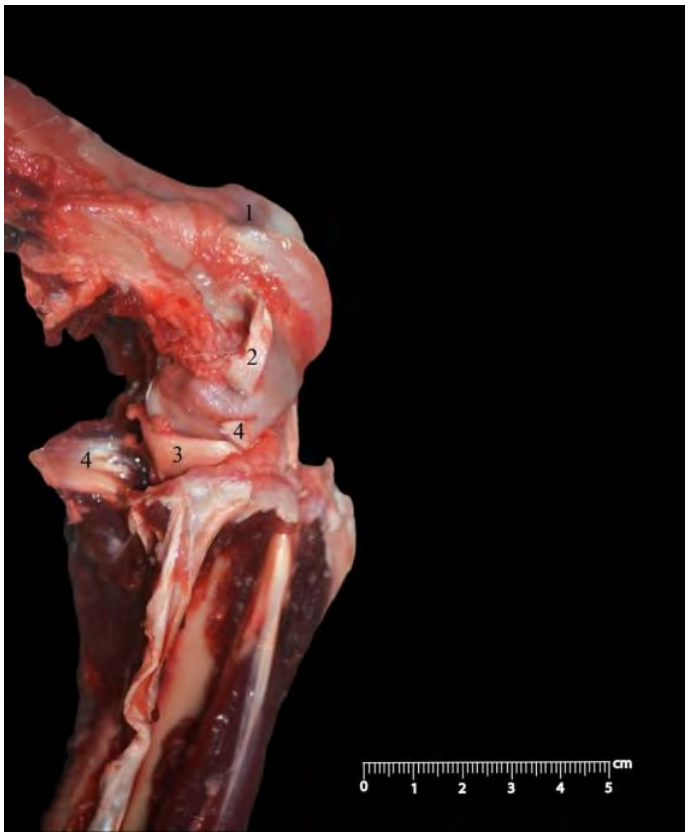

Figure 10. Lateral view of the right femur and leg of the pampas deer after removal of fasciae and gastrocnemius muscles. (**1**): Femoral trochlea; (**2**): lateral collateral ligament incised and reclined proximally; (**3**): lateral border of the lateral meniscus; (**4**): popliteus muscle transversely sectioned at the level of its tendinous part.

The patellar fibrocartilaginous apparatus (Figures 3 and 7) extended the articular surfaces of the patella and held it attached to the femoral trochlea. It consisted of two parapatellar fibrocartilages, one medial and one lateral. The medial one was slightly more developed than the lateral one.

3.3. Means of Union, Joint Capsule, and Ligaments

The means of attachment consisted of the joint capsule (*Capsula articularis*) and various ligaments (Figures 5 and 7). They can be divided into those joining the patella to the femur and tibia, and those joining the femur to the tibia.

The joint capsule was common to the entire femoropatellar joint (Figure 5). It was inserted around the distal part of the femur and around the proximal extremity of the tibia. A thin expansion was directed deep into the intercondylar fossa, covering the abaxial side of the cruciate ligaments (*Ligamenta cruciata*), which remained in an extra-articular position. The capsule cranially joined the parapatellar fibrocartilages. The femorotibial or collateral ligaments divided it into two parts: the femorotibial capsule caudally and the peripatellar capsule cranially, which is known as the patellar retinaculum in the parts distal to the patella, where it was separated into two parts, medial and lateral, by the patellar ligament.

3.4. Patellar Ligaments

There were three ligaments connected to the patella: two femoropatellar and one patellar. The femoropatellar were one medial and one lateral, very thin fascicles leading from the corresponding parapatellar fibrocartilage to the corresponding femoral epicondyle. Together with the fasciae and muscles, they held the patella cranially to the femoral trochlea (Figure 7).

The patellar ligament (*Ligamentum patellae*) (Figures 3 and 11) was thick, strong, and extended from the apex of the patella to the tibial tuberosity. This ligament represented the indirect continuation of the tendon of the quadriceps femoris muscle, transmitting its extensor action to the leg. This ligament was flattened from cranial to caudal, and each of its edges gave insertion to the retinaculae of the patella. The transverse cut shape of the patellar ligament was an ellipse. Its caudal aspect was related to the femoropatellar synovium, and distally, it was separated by the infrapatellar adipose body (*Corpus adiposum infrapatellare*), a mass of adipose tissue that was well seen on sagittal sections of the joint and on MRI scans (Figures 7 and 12). There were no other ligaments connecting the patella to the tibia.

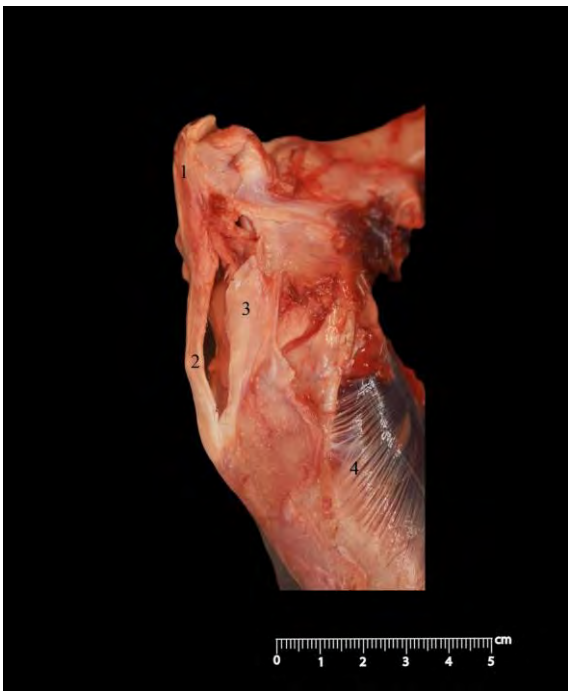

Figure 11. Medial view of the right femur and leg of the pampas deer after removal of fasciae and gastrocnemius muscles. (**1**): Patellar insertion of the patellar ligament; (**2**): patellar ligament; (**3**): articular capsule; (**4**): popliteus muscle.

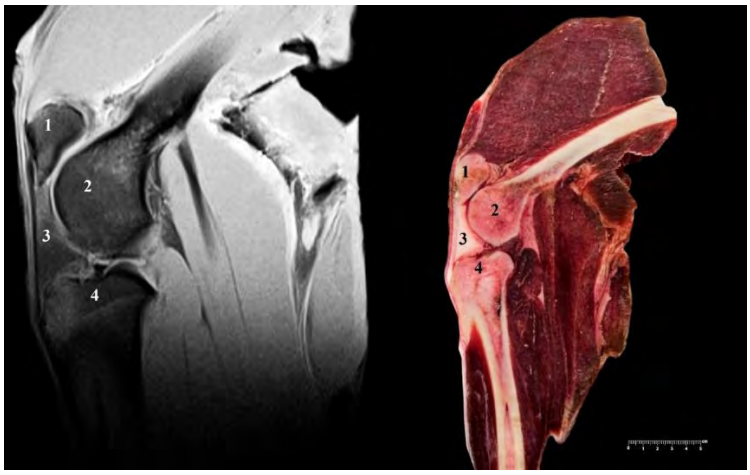

Figure 12. Left panel: MRI of the right stifle joint of the pampas deer. (**1**): Patella; (**2**): distal part of Figure 3 infrapatellar adipose body; (**4**): proximal extremity of tibia. **Right** panel: medial view of the right stifle of the pampas deer, sagittal section. (**1**): Patella; (**2**): distal part of femur; (**3**): infrapatellar adipose body; (**4**): proximal extremity of tibia.

3.5. Femorotibial Ligaments

Apart from the fibrous capsule and the femoral insertion of the meniscofemoral ligament connecting the lateral meniscus to the intercondylar fossa, there were two extra-articular cruciate ligaments and two collaterals (Figures 6, 9 and 10).

The cruciate ligaments were located adjacent to each other, separated by adipose connective tissue, and in an oblique arrangement (Figure 6). The cranial cruciate ligament (*Ligamentum cruciatum craniale*) extended from the medial aspect of the lateral condyle to the caudal intercondylar area. The caudal cruciate ligament (*Ligamentum cruciatum caudale*) extended from the intercondylar surface of the medial condyle of the femur to the popliteal incisure of the tibia, caudally to the medial articular surface, lying in the sagittal plane and crossing in "X" to the cranial cruciate ligament. These ligaments were extra-articular, interosseous, and covered on their abaxial side by the femorotibial joint capsule.

3.6. Complementary Means of Joining

The stifle joint is supported by powerful tendons that have direct relationships with the stifle joint. Caudally, the joint is covered by the gastrocnemius muscle (*M. gastrocnemius*) and the superficial digital flexor muscle (*M. flexor digitorum superficialis*). Medially, the semimembranosus, gracilis, and sartorius muscles *(M. semimembranosus, M. gracilis*, and *M. sartorius)*, as well as the fasciae, help in an important way. On the lateral side, situated the gluteobiceps muscle *(M. gluteobiceps)* and the tendon of the extensor digitorum longus toe muscle (*M. extensor digitorum longus*) (Figure 9). The latter takes its origin between the lateral condyle and the lateral lip of the trochlea, then passes through the extensor groove of the tibia and assists in joint containment. The popliteus muscle (*M. popliteus*) tendon was located laterally between the lateral meniscus and the lateral collateral ligament (Figures 9–11). Finally, on the cranial side was the insertion of the quadriceps femoris muscle (*M. quadriceps femoris*) tendon, an insertion that kept the patellar and femoropatellar ligaments taut, which helped transmit their extensor action to the leg.

3.7. Synovial

There was a synovium common to the entire femorotibiopatellar joint. The synovial fluid present inside the stifle joint was minimal in volume, transparent, and of a viscous consistency.

3.8. MRI and Simple Radiography

Bone surfaces can be easily identified in the images of all the techniques employed (Figures 8 and 12). Compact bone appeared as a hypointense signal, while cancellous bone showed heterogeneous signal intensity due to high fat content in the bone marrow and a trabecular pattern. Articular cartilage appeared as a hyperintense line that was separated from the subchondral bone by a gray line (moderate signal intensity) (Figure 12). The medial and lateral menisci showed hypodensity (Figure 12).

The medial and lateral femoropatellar ligaments as well as the meniscofemoral ligament of the lateral meniscus appeared as structures of moderate signal intensity (Figure 8). The menisci showed a very homogeneous hypointensity. The infrapatellar adipose body was very clearly and uniformly hypointense (Figure 12).

3.9. Movements

The movements performed by the joint are mainly flexion and extension, with some rotation and slight lateral movements. The tension of the ligaments, especially the cruciate ligaments, prevented other movement directions and also the hipper extension and hipper flexion of the stifle joint.

4. Discussion

Knowledge of the anatomical structures found in wild animals is important for the veterinary clinic, in surgery, and in human medicine as a laboratory model. The stifle joint is usually exposed to many problems that may require surgical treatment, such as

patellar luxation, gonitis (stifle arthritis), synovitis, fracture, meniscal tearing, and a cruciate ligament sprain in the bovine [33]. In this study, the anatomy of the femoro-tibiopatellar joint of the pampas deer is described for the first time using simple dissection and imaging as methods of study.

The overall structure of the stifle joint, including the general morphology of the joint with its bones and the presence of ligaments and the menisci, is largely conserved among all terrestrial mammals [34], and in this case, the pampas deer is no exception.

4.1. Articular Surfaces

During the dissection, it was observed that the lateral condyle of the femur was larger than the medial one, and this is similar to goat and dog, as evidenced in the study of Abumandour et al. [35].

Unlike other ruminants but especially compared to sheep, the trochlea in pampas deer was deeper, and their lips were almost symmetrical. Janis et al. [36] studied the asymmetry of the lips of the trochlea femoris in many ungulate species and mention that in species weighing less than 100 kg, there is little asymmetry. The reasons that explain the asymmetry presented by large ungulates in the trochlea femoris have not yet been found [36]. The asymmetry presented by the pampas deer is almost nonexistent, which coincides with the observation of these authors as it is a species of small size.

The bones involved in the stifle joint of the pampas deer were the femur, tibia, and patella. The patella is the largest sesamoid bone found in the animal's body, and its morphology is similar to that found in the lion [37] and the Indian muntjac [38]. In the pampas deer stifle joint, the patella was the only sesamoid bone, as in Marsh deer, free-ranging deer, or other ruminants such as cattle [22], where no other sesamoid bones were found in this joint, even when analyses were performed on radiographs. Sesamoid bones have been reported in the stifle joint of the dog [39], in the ring-tailed lemur [40], and in the gastrocnemius muscle of the paca [41].

In relation to the size of the patellar articular surfaces, it was the same as what was described for other ungulates, where the medial one was wider [24]. In general, the conformation of the bones participating in the joint was like that described for marsh deer [42].

4.2. Means of Attachment, Joint Capsule, and Ligaments

These structures were like those described in cervids [30] and small domestic ruminants [22–24].

The medial meniscus was slightly narrower and less thickened than the lateral, similar to the goat and dog, where the lateral was the largest, and more concave and thicker, contrary to the donkey, where the medial meniscus was larger than the lateral meniscus [35].

Even the menisci have not contact cranially there is not the transverse ligament of the knee which is present in the dog and sometimes in the ox, that connects the cranial angles of the two menisci [23].

The caudal horn of the lateral meniscus was divided into two parts, one inserting to the popliteal incisure of the tibia and the other to the femur, constituting the meniscofemoral ligament (Figure 8), which is different from the study of Zaino et al. [43] that the posterior horn of the lateral meniscus in the white-tailed deer knee is attached only to the femur rather than to both the tibia and femur. The caudal horn of the lateral meniscus in bovine and porcine knees is also attached only on the inner side of the medial condyle of the femur [44].

Though the menisci appear similar in size and shape to those of the human knee, it should be noted that the posterior horn of the lateral meniscus in the cervine knee is attached only to the femur (as in bovine and porcine knees) rather than to both the tibia and femur as in humans [43].

The width of the body of the medial meniscus was more uniform from cranial to caudal, while the body of the lateral meniscus became wider toward the caudal pole, quite

contrary to the study of Takroni et al. [45], where the lateral meniscus had a more uniform width from front to back while the body of the medial meniscus became wider toward the back. The caudal horn of the lateral meniscus was thickened and divided into two parts, such as in pigs [45].

The joint capsule was common to the entire femoropatellar and femorotibial joints (Figure 5) such as in swine, where the femoropatellar articulation cavity communicates distally with the femorotibial articulation. The small transverse ligament that connects the cranial edges of the menisci [33] is missing in the pampas deer knee.

The pampas deer have great capabilities for fast running, jumping, and floating in different types of terrain. These capabilities are supported anatomically by some structures such as the patellar ligament, menisci, and menisco femoral ligament, which consolidate the joint and movements between the femur and tibia. Since the pampas deer are running and jumping animals, the stability of their knee articulations can also be attributed to the femorotibial or collateral ligaments, which were divided into two parts: the femorotibial capsule caudally and the peripatellar capsule cranially known as the patellar retinaculum in the parts distal to the patella, where it was separated into two parts medial and lateral by the patellar ligament.

4.3. Imaging

Knowledge of the normal sectional anatomy of the stifle joint in the pampas deer is essential for the evaluation of images obtained by magnetic resonance imaging.

The images from the current work provide anatomical details that were compared with the corresponding macroscopic anatomical sections. Radiography is limited in its ability to evaluate soft structures. Ultrasonography can provide visualization of tendons and ligaments, but it was not used in this case.

MRI is an excellent imaging modality; however, its use in veterinary medicine is limited as it is expensive and the animal must be anesthetized. The capture and anesthesia procedures were already described and successfully tested [46]. MRI has potential advantages over routine radiography; it provides an image with superior soft tissue detail and no overlapping of structures and can be used for a better diagnosis of minor abnormalities. Signal intensities in cadaver specimens may be different from those in live animals due to fluid and blood loss, freezing, and the absence of blood circulation, but the macroscopic anatomy is the same, and the images obtained are representative of reality.

The results reveal that compact bone appears as a hypodense signal, while cancellous bone appears as a moderately dense structure. Such findings agree with Van der Straaten et al. [47] and Holcombe et al. [48] in horses. Articular cartilage shows hyperdensity, and subchondral bone has moderate signal intensity. These results agree with those of other authors [47–49].

The medial and lateral menisci showed hypodensity, a sign that was similar to what had previously been reported in other animal species [27,48]. However, Murray [50] in the horse reported that the medial and lateral menisci varied in signal intensity from moderate to low depending on the Tesla used.

The infrapatellar adipose body appears as a moderate signal in pampas deer (between hypo- and hyperdense), but was described as having a hyperdense signal that is difficult to differentiate from the synovial capsule because both appear with the same intensity [47,49].

In conclusion, the general anatomy of the stifle joint, including the overall morphology of the joint with its bones, attachments, and anatomical relationships, was similar to that of other ruminant species of similar size. Imaging techniques such as magnetic resonance imaging allow adequate visualization of most of its components.

Author Contributions: H.E.K., S.D. and W.P. contributed equally to all parts of the manuscript. All authors have read and agreed to the published version of the manuscript.

Funding: This research received no external funding.

Institutional Review Board Statement: Not applicable.

Informed Consent Statement: Not applicable.

Data Availability Statement: Data is unavailable due to privacy or ethical restrictions. If you want to have access to the data, please contact the corresponding author: durosokol@ubt.edu.al.

Acknowledgments: We thanks to Natalia Huart for her technical support.

Conflicts of Interest: The authors declare no conflict of interest.

References

1. Van Wieren, S.E. Digestive Strategies in Ruminants and Non-Ruminants. Ph.D. Thesis, University of Wageningen, Wageningen, The Netherlands, 1996.
2. Nowak, R.M.; Paradiso, J.L. *Walker's Mammals of the World*, 6th ed.; John Hopkins University: Baltimore, MD, USA, 1999; Volume 2.
3. Hackmann, T.J.; Spain, J.N. Invited review: Ruminant ecology and evolution: Perspectives useful to ruminant livestock research and production. *J. Dairy Sci.* **2010**, *93*, 1320–1334. [CrossRef]
4. González, S.; Álvarez-Valin, F.; Maldonado, J.E. Morphometric differentiation of endangered pampas deer (*Ozotoceros bezoarticus*), with description of new subspecies from Uruguay. *J. Mammal.* **2002**, *83*, 1127–1140. [CrossRef]
5. González, S.; Jackson, J.J.; Merino, M.L. *Ozotoceros bezoarticus*. The IUCN Red List of Threatened Species. 2016. Available online: https://dx.doi.org/10.2305/IUCN.UK.2016-1.RLTS.T15803A22160030.en (accessed on 18 April 2023).
6. Jackson, J.E. *Ozotoceros bezoarticus*. *Mamm. Species* **1987**, *295*, 1–5. [CrossRef]
7. Ungerfeld, R.; González-Sierra, U.T.; Piaggio, J. Reproduction in a semi-captive herd of pampas deer *Ozotoceros bezoarticus*. *Wildl. Biol.* **2008**, *14*, 350–357. [CrossRef]
8. Lingle, S. Escape gaits of white-tailed deer, mule deer, and their hybrids: Body configuration, biomechanics, and function. *Can. J. Zool.* **1993**, *71*, 708–724. [CrossRef]
9. Ungerfeld, R.; González-Pensado, S.; Bielli, A.; Villagrán, M.; Olazabal, D.; Pérez, W. Reproductive biology of the pampas deer (*Ozotoceros bezoarticus*): A review. *Acta Vet. Scand.* **2008**, *50*, 16. [CrossRef] [PubMed]
10. Pérez, W.; Vázquez, N.; Ungerfeld, R. Gross anatomy of the female genital organs of the pampas deer (*Ozotoceros bezoarticus*, Linnaeus 1758). *Anat. Histol. Embriol.* **2013**, *42*, 168–174. [CrossRef] [PubMed]
11. Pérez, W.; Vázquez, N.; Ungerfeld, R. Gross anatomy of the male genital organs of the pampas deer (*Ozotoceros bezoarticus*, Linnaeus 1758). *Anat. Sci. Int.* **2013**, *88*, 123–129. [CrossRef] [PubMed]
12. Ungerfeld, R.; Villagrán, M.; Lacuesta, L.; Vazquez, N.; Pérez, W. Asymmetrical size and functionality of the pampas deer (*Ozotoceros bezoarticus*) testes: Right testis is bigger but left testis is more efficient in spermatogenesis. *Anat. Histol. Embryol.* **2017**, *46*, 547–551. [CrossRef]
13. Pérez, W.; Clauss, M.; Ungerfeld, R. Observations on the macroscopic anatomy of the intestinal tract and its mesenteric folds in the pampas deer *(Ozotoceros bezoarticus*, Linnaeus 1758). *Anat. Histol. Embryol.* **2008**, *37*, 317–321. [CrossRef] [PubMed]
14. Pérez, W.; Ungerfeld, R. Gross anatomy of the stomach of the pampas deer, *Ozotoceros bezoarticus* (Artiodactyla: Cervidae). *Zoologia* **2012**, *29*, 337–342. [CrossRef]
15. Erdoğan, S.; Pérez, W. Anatomical and scanning electron microscopic characteristics of the tongue in the pampas deer (Cervidae: *Ozotoceros bezoarticus*, Linnaeus 1758). *Microsc. Res. Tech.* **2013**, *76*, 1025–1034. [CrossRef]
16. Pérez, W.; Vazquez, N.; Ungerfeld, R. Arterial vascularization of the gastrointestinal tract of the pampas deer (*Ozotoceros bezoarticus*, Linnaeus, 1758). *Anat. Histol. Embryol.* **2016**, *45*, 240–245. [CrossRef]
17. Pérez, W.; Erdoğan, S. Arterial thoracic vascularization in some deer species: Pampas deer (*Ozotoceros bezoarticus*), brown brocket deer (*Mazama gouazoubira*) and axis deer (*Axis axis*). *Anat. Histol. Embryol.* **2014**, *43*, 490–494. [CrossRef]
18. Vazquez, N.; Ríos, C.; Sorriba, V.; Pérez, W. Arterial distribution to the pelvic cavity and pelvic limb in the pampas deer (*Ozotoceros bezoarticus*, Linnaeus 1758). *Anat. Histol. Embryol.* **2018**, *47*, 133–139. [CrossRef]
19. Vazquez, N.; Dos Santos, D.; Pérez, W. Arterial irrigation of the head and neck of the pampas deer (*Ozotoceros bezoarticus*, Linnaeus 1758). *Anat. Sci. Int.* **2018**, *93*, 540–547. [CrossRef] [PubMed]
20. Vazquez, N.; Dos Santos, D.; Pérez, W.; Artigas, R.; Sorriba, V. Gross Anatomy of the Heart of Pampas Deer (*Ozotoceros bezoarticus*, Linnaeus 1758). *J. Morphol. Sci.* **2019**, *36*, 190–195. [CrossRef]
21. Allen, M.J.; Houlton, J.E.; Adams, S.B.; Rushton, N. The surgical anatomy of the stifle joint in sheep. *Vet. Surg.* **1998**, *27*, 596–605. [CrossRef]
22. Getty, R. *Sisson and Grossman's the Anatomy of the Domestic Animals*, 5th ed.; Saunders: Philadelphia, PA, USA, 1975.
23. Nickel, R.; Schummer, A.; Seiferle, E.; Frewein, J.; Wilkens, H.; Wille, K.H. *The Locomotor System of the Domestic Mammals*; Paul Parey: Berlin, Germany; Hamburg, Germany, 1986.
24. Barone, R. *Anatomie Comparée des Mammifères Domestiques, Tome 2: Arthrologie et Myologie*, 4th ed.; Vigot: Paris, France, 2010.
25. Foreman, J.H. Use of magnetic resonance imaging in equine lameness diagnosis. *Pferdeheilkunde* **1996**, *12*, 686–687. [CrossRef]
26. Gavin, P.; Holmes, S. Stifle Joint. In *Practical Small Animal MRI*; Gavin, P.R., Bagley, R.S., Eds.; Wiley-Blackwell: Ames, IA, USA, 2009; pp. 233–273.
27. Cook, C. MRI of the canine stifle joint. In Proceedings of the 3rd World Veterinary Orthopaedic Congress and 15th European Society of Veterinary Orthopaedics and Traumatology Congress (ESVOT-VOS), Bologna, Italy, 15–18 September 2010.

28. Mair, S.; Lattermann, C.; Malone, T.R. Glenohumeral instability and glenoid bone loss in a throwing athlete. *Int. J. Sports Phys. Ther.* **2013**, *8*, 205–211. [PubMed]
29. Vandeweerd, J.M.; Kirschvink, N.; Muylkens, B.; Cintas, C.; Catsyne, C.V.; Hontoir, F.; Clegg, P.; Coomer, R.; Nisolle, J.F. Magnetic resonance imaging (MRI) anatomy of the ovine stifle. *Vet. Surg.* **2013**, *42*, 551–558. [CrossRef] [PubMed]
30. Shigue, D.A.; Rahal, S.C.; Schimming, B.C.; Santos, R.R.; Vulcano, L.C.; Linardi, J.L.; Teixeira, C.R. Evaluation of the marsh deer stifle joint by imaging studies and gross anatomy. *Anat. Histol. Embryol.* **2015**, *44*, 468–474. [CrossRef] [PubMed]
31. International Committee on Veterinary Gross Anatomical Nomenclature. *Nomina Anatomica Veterinaria*, 6th ed.; World Association of Veterinary Anatomists: Hanover, Germany, 2017.
32. Constantinescu, G.M. *Illustrated Veterinary Anatomical Nomenclature*, 4th ed.; Thieme: Stuttgart, Germany, 2018.
33. Weaver, A.D.; St. Jean, G.; Steiner, A. Lameness. In *Bovine Surgery and Lameness*, 2nd ed.; Blackwell Publishing: Oxford, UK; Ames, IA, USA; Carlton, Australia, 2005.
34. Mancini, I.A.D.; Rieppo, L.; Pouran, B.; Afara, I.O.; Braganca, F.S.; van Rijen, M.H.P.; Kik, M.; Weinans, H.; Toyras, J.; van Weeren, P.R.; et al. Effects of body mass on microstructural features of the osteochondral unit: A comparative analysis of 37 mammalian species. *Bone* **2019**, *127*, 664–673. [CrossRef] [PubMed]
35. Abumandour, M.; Bassuoni, N.F.; El-Gendy, S.; Karkoura, A.; El-Bakary, R. Comparative Morphological Studies of the Stifle Menisci in Donkeys, Goats and Dogs. *J. Morphol. Sci.* **2019**, *36*, 72–84. [CrossRef]
36. Janis, C.M.; Shoshitaishvili, B.; Kambic, R.; Figueirido, B. On their knees: Distal femur asymmetry in ungulates and its relationship to body size and locomotion. *J. Vertebr. Paleontol.* **2012**, *32*, 433–445. [CrossRef]
37. Kirberger, R.M.; du Plessis, W.M.; Turner, P.H. Radiologic anatomy of the normal appendicular skeleton of the lion (*Panthera leo*). Part 2: Pelvic limb. *J. Zoo Wildl. Med.* **2005**, *36*, 29–35. [CrossRef]
38. Rajani, C.V.; Chandrasekhar, L.; Chandy, G.; Chungath, J.J. Anatomical studies on the bones of the pelvic limb in Indian muntjac (*Muntiacus muntjak*). *Tamilnadu J. Vet. Anim. Sci.* **2013**, *44*, 21–25.
39. Evans, H.E.; De Lahunta, A. *Miller's Anatomy of the Dog*; Elsevier: St. Louis, MO, USA, 2013.
40. Makungu, M.; Groenewald, H.B.; Du Plessis, W.M.; Barrows, M.; Koeppel, K.N. Osteology and Radiographic Anatomy of the Pelvis and Hind Limb of Healthy Ring-Tailed Lemurs (*Lemur catta*). *Anat. Histol. Embryol.* **2014**, *43*, 190–202. [CrossRef]
41. de Araújo, F.A.P.; Sesoko, N.F.; Rahal, S.C.; Teixeira, C.R.; Müller, T.R.; Machado, M.R.F. Bone morphology of the hind limbs in two caviomorph rodents. *Anat. Histol. Embryol.* **2013**, *42*, 114–123. [CrossRef]
42. Schimming, B.C.; Rahal, S.C.; Shigue, D.A.; Linardi, J.L.; Vulcano, L.C.; Teixeira, C.R. Osteology and radiographic anatomy of the hind limbs in Marsh deer (*Blastocerus dichotomus*). *Pesq. Vet. Bras.* **2015**, *35*, 997–1001. [CrossRef]
43. Zaino, N.L.; Hedgeland, M.J.; Ciani, M.J.; Clark, A.M.; Kuxhaus, L.; Michalek, A.J. White-Tailed Deer as an Ex Vivo Knee Model: Joint Morphometry and ACL Rupture Strength. *Ann. Biomed. Eng.* **2017**, *45*, 1093–1100. [CrossRef] [PubMed]
44. Proffen, B.L.; McElfresh, M.; Fleming, B.C.; Murray, M.M. A comparative anatomical study of the human knee and six animal species. *Knee* **2012**, *19*, 493–499. [CrossRef] [PubMed]
45. Takroni, T.; Laouar, L.; Adesida, A.; Elliott, J.A.; Jomha, N.M. Anatomical study: Comparing the human, sheep and pig knee meniscus. *J. Exp. Orthop.* **2016**, *3*, 35. [CrossRef] [PubMed]
46. Fumagalli, F.; Villagrán, M.; Ungerfeld, R. The repetition of semen collection does not affect the physiological and biochemical response to electroejaculation of anesthetized adult and yearling pampas deer (*Ozotoceros bezoarticus*) males. *Emerg. Anim. Species* **2022**, *4*, 100010. [CrossRef]
47. Van der Straaten, G.O. Magnetic Resonance Imaging of the Equine Stifle: Normal Anatomy. Master's Thesis, University of Utrecht, Utrecht, The Netherlands, 2009.
48. Holcombe, S.J.; Bertone, A.L.; Biller, D.S.; Haider, V. Magnetic resonance imaging of the equine stifle. *Vet. Radiol. Ultrasound* **1995**, *36*, 119–125. [CrossRef]
49. Soler, M.; Murciano, J.; Latorre, R.; Belda, E.; Rodrı, M.J.; Agut, A. Ultrasonographic, computed tomographic and magnetic resonance imaging anatomy of the normal canine stifle joint. *Vet. J.* **2007**, *174*, 351–361. [CrossRef] [PubMed]
50. Murray, R.C. (Ed.) *Equine MRI*; John Wiley: New York, NY, USA, 2010.